FEBS 26030 FEBS Letters 517 (2002) 267–271

Identification of residues important for NAD$^+$ binding by the *Thermotoga maritima* α-glucosidase AglA, a member of glycoside hydrolase family 4

Carsten Raasch[a], Martin Armbrecht[a], Wolfgang Streit[a], Birte Höcker[b], Norbert Sträter[c], Wolfgang Liebl[a,*]

[a] *Institut für Mikrobiologie und Genetik, Georg-August-Universität, Grisebachstr. 8, D-37077 Göttingen, Germany*
[b] *Institut für Biochemie, Universität zu Köln, Cologne, Germany*
[c] *Institut für Chemie, Freie Universität Berlin, Berlin, Germany*

Received 31 January 2002; revised 21 March 2002; accepted 23 March 2002

First published online 4 April 2002

Edited by Judit Ovádi

Abstract The NAD$^+$-requiring enzymes of glycoside hydrolase family 4 (GHF4) contain a region with a conserved Gly-XXX-Gly-Ser (GXGS) motif near their N-termini that is reminiscent of the fingerprint region of the Rossmann fold, a conserved structural motif of classical nicotinamide nucleotide-binding proteins. The function of this putative NAD$^+$-binding motif in the α-glucosidase AglA of *Thermotoga maritima* was probed by directed mutagenesis. The K_d for NAD$^+$ of the AglA mutants G10A, G12A and S13A was increased by about 300-, 5-, and 9-fold, respectively, while their K_m for *p*-nitrophenyl-α-glucopyranoside was not seriously affected. The results indicate that the GXGS motif is indeed important for NAD$^+$ binding by the glycosidases of GHF4. © 2002 Published by Elsevier Science B.V. on behalf of the Federation of European Biochemical Societies.

Key words: α-Glucosidase; Cofactor; NAD$^+$ binding; Rossmann fold; Site-directed mutagenesis; *Thermotoga maritima*

1. Introduction

Glycoside hydrolase family 4 (GHF4) is a family of glycosidic bond-cleaving enzymes which are related by similarity of their amino acid sequences [1,2]. Enzymes with various reaction specificities are found in this family, i.e. α-galactosidases (EC 3.2.1.22; e.g. MelA of *Escherichia coli* [3]), α-glucosidases (EC 3.2.1.20; e.g. AglA of *Thermotoga maritima* and *Thermotoga neapolitana* [4,5]), 6-phospho-β-glucosidases (EC 3.2.1.86; e.g. the CelF proteins of *E. coli* and *Bacillus subtilis* [6]), and 6-phospho-α-glucosidases (EC 3.2.1.122; e.g. GlvA of *B. subtilis*, AglB of *Klebsiella pneumoniae*, and the MalH of *Fusobacterium mortiferum* [7–9]). Interestingly, some enzymes of this family are specific for α-glycosidic bonds while others display β specificity during cleavage. All other GHF families contain either α- or β-specific glycosidases. Also, it is noteworthy that no eukaryal or archaeal members of this unique enzyme type are known.

The common features of GHF4 enzymes, where investigated so far, may be summarized as follows (see [4]): (i) relative instability of the enzymes; (ii) requirement of Mn^{2+} (or Co^{2+}, Ni^{2+} or Fe^{2+}) for activity; (iii) requirement of NAD$^+$ for activity; (iv) oligomeric quaternary structure (homodimer or -tetramer); (v) subunit size about 51 kDa (about 450 residues); (vi) glycone specificity for glucose, its C4 epimer galactose or both, or for glucose 6-phosphate [3,4,6–8].

NAD$^+$ activation is the exception in glycoside hydrolases and has been found only in GHF4 enzymes while the majority of glycoside hydrolases, including many other intracellular oligosaccharidases, are not activated by NAD$^+$. The role of NAD$^+$ for the activity of the hydrolytic enzymes of GHF4 is not understood. Spectrophotometric measurements failed to detect the conversion of NAD$^+$ to NADH by GHF4 enzymes ([6,8], and own unpublished data). Three-dimensional structures of GHF4 enzymes, which could shed light on their unusual cofactor dependence, have not been reported. The pyridine nucleotide cofactor could have structural and/or catalytic function and, in addition, could also be important for regulation of enzyme activity (see [4]).

The α-glucosidase AglA from the hyperthermophilic bacterium *T. maritima* represents a thermostable GHF4 member. This enzyme requires NAD$^+$, Mn^{2+}, and a relatively high concentration of thiol-containing reducing agents like dithiothreitol for activity [4,10]. The primary structures of the AglA enzymes from *T. maritima* and the related species *T. neapolitana* share only low-level similarity (up to about 26% identity) with the other GHF4 enzymes. Interestingly, however, the N-terminus of AglA carries a motif of residues which is conserved throughout GHF4 ([8]; own unpublished data) and which is reminiscent of a 'fingerprint' sequence pattern found in many of the classical nicotinamide dinucleotide-binding enzymes, most of which are oxidoreductases [11,12]. In order to determine if the conserved sequence motif of GHF4 enzymes is indeed involved in dinucleotide binding, we decided to study the effect of amino acid substitutions in this motif on the activity and apparent NAD$^+$-binding affinity of *T. maritima* AglA.

2. Materials and methods

2.1. General DNA modification methods and in vitro mutagenesis of the aglA open reading frame

Recombinant DNA techniques and expression of the recombinant gene were performed in *E. coli* XL1-Blue and BL21(DE3), respec-

*Corresponding author. Fax: (49)-551-394897.
E-mail address: wliebl@gwdg.de (W. Liebl).

0014-5793/02/$22.00 © 2002 Published by Elsevier Science B.V. on behalf of the Federation of European Biochemical Societies.
PII: S0014-5793(02)02641-8

tively. *E. coli* strains were routinely grown in Luria–Bertani (LB) broth supplemented with ampicillin (100 μg ml^{-1}). DNA manipulations were done according to standard protocols [13]. Polymerase chain reaction (PCR)-mediated amplification of the *aglA* open reading frame (ORF) was done with the following primers: wt-for: 5′-GGAGGAATTCATGCCATCTGTGAAGATCGGTA-3′; wt-rev: 5′-CAGAAGCTTTCATCTCTTCAGATAATGTTTCCG-3′. The *Eco*RI and *Hin*dIII restriction sites, respectively, which were used for cloning of the PCR product are underlined. For in vitro mutagenesis of *aglA*, the following mutagenic PCR primers were used which span the 5′ end of the *aglA* ORF from the ATG start codon to the mutagenesis target sites at codons 10–13 (mutagenic positions in bold): G10A-for: 5′-GGAGGAATTCATGCCATCTGTGAAGATCGGTATCATCG**C**TGCGGGGAGC-3′; G12A-for: 5′-GGAGGAATTCATGCCATCTGTGAAGATCGGTATCATCGG-TGCGG**C**GAGCGCGGTG-3′; S13A-for: 5′-GGAGGAATTCATGCCATCTGTGAAGATCGGTATCATCGGTGCGGGG**GC**CGCGGTGTTTTC-3′. The wild type and mutated *aglA* ORFs were generated by PCR reactions with the mutagenic primers, using wt-rev as the reverse primer in all cases. The *aglA*-containing plasmid pWBE2.4 [4] served as the template DNA. Reaction mixtures (50 μl) contained 125 pmol each of the forward and reverse primers, 0.2 μg template DNA, 1.25 mM each of the four dNTPs, 5 μl dimethyl sulfoxide, 5 μl 10× *Pfu* reaction buffer, and 4.5 U *Pfu* DNA polymerase. The template DNA was denatured for 5 min at 94°C, followed by 32 amplification cycles (45 s at 94°C, 45 s at 38°C, 2 min at 72°C) and finally 10 min at 72°C. The PCR products were cloned into *Eco*RV-linearized pBluescript SK$^+$, excised from the resulting plasmids with *Eco*RI and *Hin*dIII and ligated downstream of the P_{T7} promoter into the correspondingly cut expression vector pET21a. The resulting α-glucosidase expression plasmids pET21a-AglA, pET21a-G10A, pET21a-G12A, and pET21a-S12A were transformed into *E. coli* BL21(DE3).

2.2. Purification of recombinant α-glucosidase and α-glucosidase mutants

AglA and its derivatives were produced recombinantly by growing *E. coli* BL21(DE3) strains transformed with pET21a-AglA, pET21a-G10A, pET21a-G12A, and pET21a-S12A with aeration at 37°C in LB broth containing 100 μg ml^{-1} ampicillin. At OD_{600nm} = 0.5–0.6, 0.3 mM IPTG was added, and incubation was continued for 5 h. Cells were harvested, washed with 20 mM Tris–HCl pH 8.0, resuspended in a small volume of the same buffer and disrupted by repeated passage through a French pressure cell (American Instrument Company, Silver Spring, OH, USA) at 6.9 MPa. After centrifugation (40 000 × *g*, 30 min, 4°C) the cleared homogenate was incubated at 75°C for 15 min and cooled on ice. Precipitated proteins were sedimented (40 000 × *g*, 30 min, 4°C), and the supernatant was subjected to anion exchange chromatography on a 50 ml bed volume Source 15 Q column (XK26, Pharmacia, Freiburg, Germany), employing a linear 0.1–0.4 M NaCl gradient in 20 mM Tris–HCl pH 8.0 for elution. Fractions containing the α-glucosidase proteins were pooled, dialyzed against 50 mM Tris–HCl pH 7.5, and concentrated by ultrafiltration (30 kDa cutoff). During all steps of the purification protocol, the mutant enzymes AglA-G10A, AglA-G12A and AglA-S13A behaved in a manner indistinguishable from the wild type enzyme.

2.3. Enzyme assays and analytical methods

The standard α-glucosidase assay was based on the enzymatic liberation of nitrophenol from *para*-nitrophenyl-α-D-glucoside (pNP-α-Glc). Assay mixtures (300 μl) contained 50 mM Tris–HCl pH 7.0, 1 mM $MnCl_2$, 1.8 mM NAD$^+$, 50 mM dithiothreitol, and enzyme. After pre-equilibration for 5 min at 60°C the reaction was started by addition of 10 μl 0.1 M pNP-α-Glc, and incubation was continued for 4–20 min. Within this range, the assay had a linear time dependence of product formation. The reaction was cooled on ice, mixed with 20 μl 0.5 M EDTA pH 8.0 and 680 μl water, and the absorbance was measured at 420 nm. The molar extinction coefficient of pNP under these conditions was 12 000 M^{-1} cm^{-1}. One unit of enzyme released 1 μmol of pNP in 1 min under the specified conditions. The same assay method, with modifications as described in the text, was used for kinetic analyses. The enzyme concentrations used were 5.1–7.6 μg ml^{-1} (AglA-wt), 35–72 μg ml^{-1} (AglA-G10A), 3.9–5.9 μg ml^{-1} (AglA-G12A), and 14.7–29.5 μg ml^{-1} (AglA-S13A). For the determination of the K_m for pNP-α-Glc and the K_d (approx.) for NAD$^+$, the initial velocity of pNP-α-Glc cleavage was measured at fixed, near-saturating concentrations of NAD$^+$ or pNP-α-Glc, respectively. The rate of pNP liberated was plotted as a function of the rate divided by the pNP-α-Glc or NAD$^+$ concentration, respectively, and the kinetic constants were estimated graphically from the intercepts of the Eadie–Hofstee plots at the ordinate (V_{max}) and the abscissa (V_{max}/K_m). All experiments were performed at least in duplicate.

Protein concentrations were determined at 280 nm via the specific molar absorption coefficient of AglA (1.8 l g^{-1} cm^{-1}) calculated from the amino acid composition as described by Pace et al. [14]. Fluorescence emission spectra were measured with a F-4500 spectrofluorimeter (Hitachi) at λ_{exc} = 280 nm and 295 nm. Circular dichroism (CD) spectroscopy was carried out with a J-720 spectropolarimeter (Jasco) in the near-UV (250–310 nm) and far-UV range (200–250 nm) at protein concentrations of 3.7–8.2 mg ml^{-1} and 0.53–0.66 mg ml^{-1}, respectively, using 0.1 cm quartz cuvettes. The CD spectra were recorded by five time (near-UV) or 10 time (far-UV) accumulation.

3. Results and discussion

3.1. Conserved amino acid residues and structural features of the N-termini of GHF4 enzymes

Fig. 1 shows an alignment of the N-termini of a selection of GHF4 enzymes and compares these sequences with the fingerprint motif of the coenzyme-binding region of classical NAD$^+$-dependent oxidoreductases and UDP-galactose 4-epimerase. This fingerprint region is part of the well-known 'Rossmann' fold, a conserved structural motif of nicotinamide dinucleotide-binding proteins [11,15]. This fold represents an alternating β-strand–α-helix motif with the pattern βαβαβ and is involved in the binding of the cofactor in a specific orientation and conformation. The fingerprint region has the following characteristics [12,16]. (1) A conserved positively charged residue at the amino-terminus of the first β strand. (2) A glycine-rich sequence, GXGXXG (where X are variable residues), which forms a loop connecting the first β-strand and the first α-helix. This part is important for binding of the diphosphate of the dinucleotide. The first glycine allows for a tight turn of the main chain, and the lack of a side chain at the second glycine is thought to allow for a close association between the diphosphate moiety and the main chain. The third glycine, which is often replaced by other amino acids (alanine, serine, proline) in NADP$^+$-dependent enzymes, is of importance for the close packing of the first β-strand and the first α-helix. (3) A hydrophobic core consisting of six hydrophobic residues which are important for interactions between the secondary structure elements, i.e. the packing of the β-strands against the α-helix. (4) A conserved negatively charged residue at the carboxy-terminus of the second β-strand which binds to the ribose 2′-hydroxyl of the adenine moiety of the dinucleotide. Some exceptions to each of these recurring themes are tolerated, however (see [12]).

A characteristic pattern of conserved positions strikingly similar to the Rossmann fold fingerprint pattern outlined above can be found near the N-termini of GHF4 enzymes, including a core region with conserved hydrophobic residues flanked by a positively charged residue N-terminal to the first β-strand and a negatively charged residue at the C-terminal end of the second β-strand, as well as strictly conserved glycine residues after the first β-strand (Fig. 1). However, the alignment shown in Fig. 1 also points out some obvious differences between the GHF4 N-terminal motif and the classical Rossmann fold fingerprint region: (1) the fingerprint region of GHF4 is longer than the Rossmann fold motif; this could be the result of slightly longer secondary structure elements or

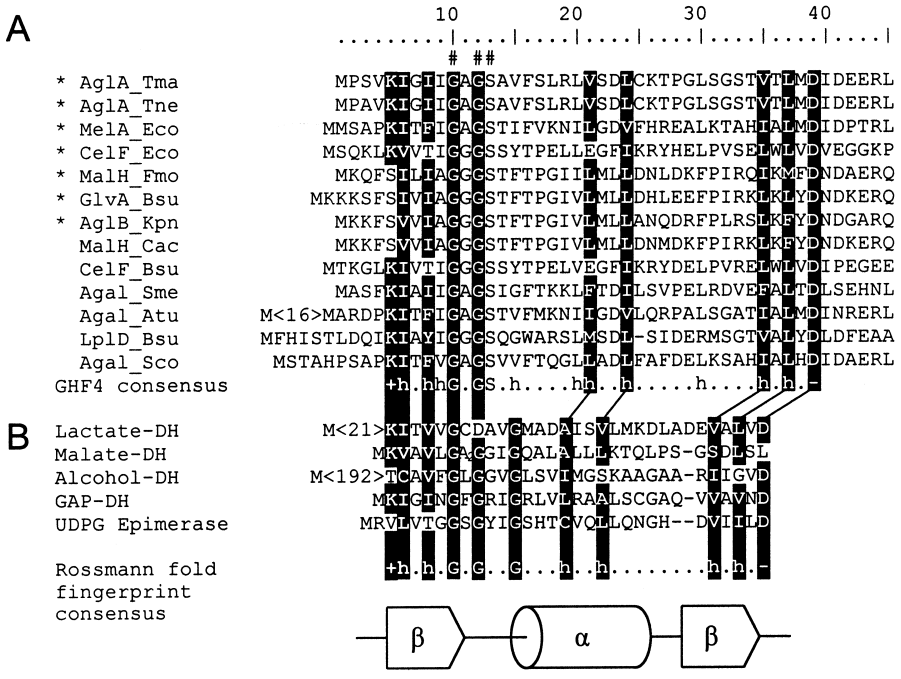

Fig. 1. Sequence similarity between the N-termini of GHF4 enzymes and the fingerprint region of the Rossmann fold. A: Alignment of N-terminal amino acid sequences of selected enzymes of GHF4. Enzymes marked with an asterisk have been shown experimentally to be NAD^+-dependent. Residues listed in the 'consensus' line are those recognized as conserved hydrophobic (h), positively charged (+) or negatively charged (−) positions. The residues mutagenized in *T. maritima* AglA in this study are marked with # symbols. B: Fingerprint region of classical NAD^+-binding proteins with known three-dimensional structures. Structurally conserved hydrophobic (h) or charged (+, −) positions are marked according to Bellamacina et al. [12]. At the bottom, the approximate extensions of characteristic secondary structure elements of the Rossmann fold are indicated. Abbreviations in alphabetical order (amino acid sequence accession numbers in parentheses): Agal_Atu, putative α-galactosidase from *Agrobacterium tumefaciens* (AAK88782); Agal_Sme, putative α-galactosidase from *Sinorhizobium meliloti* (Q9X4Y0); AglA_Tma, α-glucosidase AglA from *T. maritima* (CAA04524); AglA_Tne, α-glucosidase AglA from *T. neapolitana* (CAA08868); AglB_Kpn, 6-phospho-α-glucosidase AglB from *K. pneumoniae* (AAK01457); CelF_Bsu, 6-phospho-β-glucosidase CelF from *B. subtilis* (P46320); CelF_Eco, 6-phospho-β-glucosidase CelF from *E. coli* (P17411); agal_Sco, putative galactosidase from *Streptomyces coelicolor* (CAB59598); GlvA_Bsu, 6-phospho-α-glucosidase GlvA from *B. subtilis* (P54716); LplD_Bsu, putative hydrolase from *B. subtilis* (P39130); MalH_Cac, putative 6-phospho-α-glucosidase MalH from *Clostridium acetobutylicum* (AAK69556); MalH_Fmo, 6-phospho-α-glucosidase MalH from *F. mortiferum* (O06901); MelA_Eco, α-galactosidase MelA from *E. coli* (P06720).

longer connecting loops in the GHF4 N-terminal motif; (2) the last glycine residue in the GXGXXG motif is not conserved in the GHF4 amino acid sequences. Instead, these enzymes contain the highly conserved sequence GXGS (residues 10–13 in the *T. maritima* AglA sequence). It is noteworthy that the GXGS motif is located within the most conserved part of the GHF4 enzymes which is their N-terminal half (about 220 residues), as found by multiple sequence alignments with CLUSTAL W (data not shown).

The presence of a possible dinucleotide binding motif at the N-terminus of GHF4 enzymes has also been suggested by Thompson et al. [8]. The observation that mutagenesis of the residue Asp41 of GlvA from *B. subtilis* (corresponds to Asp39 of *T. maritima* AglA), which is situated at the end of the postulated NAD^+-binding motif shown in Fig. 1, led to an enzyme with reduced activity [8] was in agreement with this postulate. However, the reason for the loss of activity was not studied in detail, so it is not clear whether this was indeed a consequence of impaired dinucleotide binding by the mutant enzyme or if a different effect (e.g. impaired binding of the metal ion cofactor, impaired substrate binding, misfolding of the polypeptide chain) could have caused enzyme inactivation.

3.2. Site-directed mutagenesis of the putative NAD^+-binding motif of AglA

The conserved glycine residues G10 and G12, and a conserved serine S13 of the GXGS motif of AglA were replaced by alanine via site-directed mutagenesis of the corresponding codons of the *aglA* open reading frame. The mutations were confirmed by nucleotide sequence analysis. The sequences encoding AglA and its mutated derivatives were used for construction of the α-glucosidase expression plasmids pET21a-AglA, pET21a-G10A, pET21a-G12A, and pET21a-S12A (see Section 2), and high-level, IPTG-inducible P_{T7} promoter-driven expression was achieved with these plasmids in *E. coli* BL21(DE3). AglA and its variants AglA-G10A, AglA-G12A and AglA-S13A were purified from crude extracts of the recombinant *E. coli* strains as described in Section 2. All four enzymes were obtained in yields of about 10–15 mg l^{-1} culture and were >95% pure as judged by SDS–PAGE analysis (data not shown). All mutant proteins displayed pNP-α-D-glucopyranoside-hydrolyzing activity, but the activities of AglA-G10A and AglA-S13A were significantly reduced (see Table 1).

Since replacement of a glycine residue by a different amino acid invariably means that a bulkier side chain is introduced, it was important to check if the mutations caused significant disturbances in the secondary or tertiary structure of the enzymes. Therefore, the mutant AglA derivatives were subjected to fluorescence spectroscopy and CD spectroscopy, and their spectral characteristics were compared to the wild type enzyme. The near-UV range CD spectrum depends strongly

on the environment of aromatic residues, whereas the far-UV CD spectrum is dominated by the peptide bonds. Therefore, near-UV and far-UV CD spectra provide specific information on the integrity of the tertiary and secondary structure of a protein, respectively [17]. The CD spectra recorded for wild type AglA and the mutant proteins AglA-G10A, AglA-G12A and AglA-S13A in the far-UV (200–250 nm) and in the near-UV range (250–310 nm) are very similar, proving that no significant structural perturbation is caused by the introduced amino acid exchanges (Fig. 2). Along these lines, no differences were observed in the shapes and maxima of the fluorescence emission spectra recorded for all four enzymes at excitation wavelengths of 280 nm and 295 nm (data not shown). Also, the observation that the behavior of the AglA mutants during protein purification was indistinguishable from the wild type enzyme and the fact that all mutant enzymes displayed α-glucosidase activity (see above) argue against dramatic changes in the overall three-dimensional structure. Taken together, these data indicate that the mutations had no major effect on the fold of AglA.

If the GXGS motif of AglA is indeed involved in NAD^+ binding in a similar way as found at the Rossmann fold in classical dinucleotide-dependent enzymes, then one should expect this motif to be located in a short loop connecting a β-strand and an α-helix (βA and αB) at the surface of the dinucleotide-binding cleft (see [12]). In that case, there should be sufficient space to accommodate a larger side chain, like the methyl group of alanine upon replacement of glycine as in the G10A and G12A mutants, while major changes in the fold of the protein chain are not to be expected.

3.3. Kinetic parameters of AglA and the AglA mutants

Kinetic data of pNP-α-D-glucopyranoside cleavage were gathered for all enzymes by varying the substrate concentration between 0.05 mM and 10 mM, using a fixed NAD^+ concentration of 1.8 mM (for AglA-wt, AglA-G12A and AglA-S13A) or 50 mM (for AglA-G10A, which has a drastically increased apparent K_d for NAD^+). The apparent dissociation constant for NAD^+ was determined at a fixed pNP-α-D-glucopyranoside concentration of 3.3 mM. Initial reaction velocities were measured at NAD^+ concentrations in the range of 0.05–3 mM for AglA-G12A and AglA-S13A, and in the range of 1–30 mM for AglA-G10A. A typical Michaelis–Menten-like hyperbolic relationship between the NAD^+ concentration and the reaction velocity was found. The results of the kinetic characterization of the enzymes are summarized in Table 1.

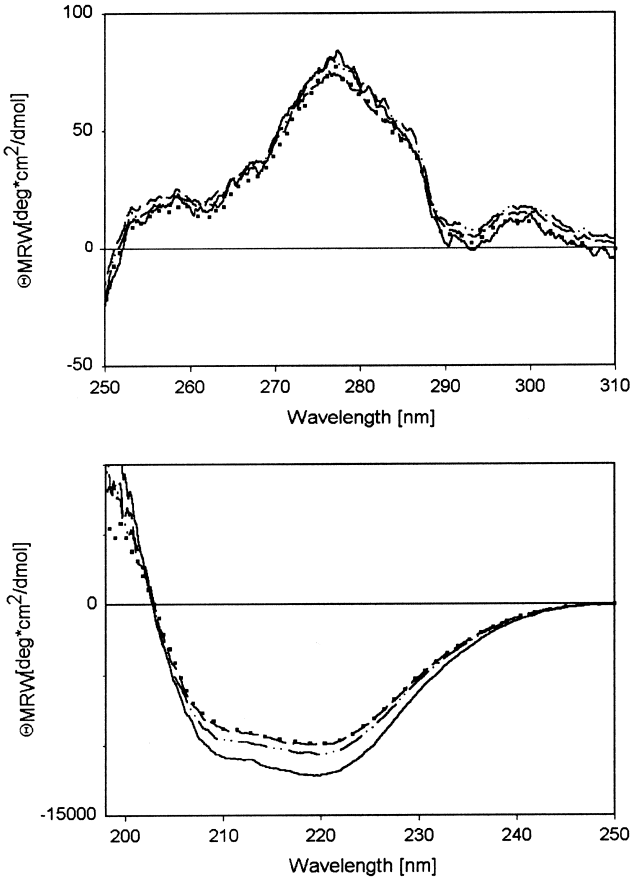

Fig. 2. Near-UV (top graph) and far-UV CD spectra (bottom graph) of AglA and its mutant variants. The CD spectra of AglA-wt (solid line), AglA-G10A (dashed line), AglA-G12A (dotted line), and AglA-S13A (dash-dotted line) were recorded by five time (near-UV) or 10 time (far-UV) accumulation at protein concentrations of 3.7–8.2 mg ml^{-1} (near-UV) and 0.53–0.66 mg ml^{-1} (far-UV), using 0.1 cm quartz cuvettes.

All mutations introduced into the GXGS motif of *T. maritima* AglA led to a reduction (5–~300-fold) of the apparent binding affinity for NAD^+ (Table 1). The S13A mutant had

Table 1
Kinetic parameters of native AglA and mutant enzymes

	K_d (NAD^+) [mM]	K_d [mutant:wild type]	k_{cat} [min^{-1}]
Kinetic parameters at a fixed concentration (3.3 mM) of pNP-α-Glc:			
AglA-wt	0.04 ± 0.01	1	202 ± 4
AglA-G10A	11.8 ± 1.5	295	121 ± 9
AglA-G12A	0.20 ± 0.01	5	245 ± 3
AglA-S13A	0.37 ± 0.01	9	34 ± 3
	K_m (pNP-α-Glc) [mM]	K_m [mutant:wild type]	k^a_{cat} [min^{-1}]
Kinetic parameters at a fixed concentration (1.8 mM or 50 mM) of NAD^+[b]:			
AglA-wt	0.23 ± 0.02	1.0	199 ± 2
AglA-G10A	0.21 ± 0.02	1.0	90 ± 2
AglA-G12A	0.19 ± 0.02	0.8	220 ± 9
AglA-S13A	0.28 ± 0.01	1.2	31 ± 1

[a]The slightly lower k_{cat} values of this series of experiments compared to the k_{cat} values given above may be due to the general instability and oxygen sensitivity of AglA [4], as not all assays were done on the same day. Also, note that the K_m of AglA-G10A was determined at 50 mM NAD^+ (merely about four-fold K_d), leading to a slightly lower velocity than expected according to Michaelis–Menten theory.
[b]At 1.8 mM for AglA-wt, AglA-G12A, and AglA-S13A, at 50 mM for AglA-G10A.

suffered a nine-fold increase of K_d and simultaneously a six-fold reduction of k_{cat}, whereas for the G12A mutant the observed five-fold increase of K_d was not accompanied by a great change in k_{cat}. The most dramatic effect on the binding affinity for the cofactor NAD^+ was observed for the G10A mutant, where the K_d for NAD^+ increased about 300-fold compared to the wild type enzyme. This enzyme variant also suffered a moderate decrease of k_{cat} to about 45–60% of the wild type level. On the other hand, the K_m values for pNP-α-D-glucopyranoside of the mutants (determined at a NAD^+ concentration of 1.8 mM for G12A and S13A, and at 50 mM for G10A) were close to the Michaelis constant of the wild type enzyme, which means that the mutations introduced into AglA did not seriously affect the integrity of the substrate binding region.

Obviously, all mutations analyzed here affect NAD^+ binding but do not completely destroy the binding pocket or prevent binding by steric repulsion. Most likely, these mutations will influence the orientation of the NAD^+, so they can primarily be interpreted as 'positional mutations' of the NAD^+ and its contribution to catalysis. Of course, the possibility that mutations also affect other residues cannot be excluded. Two mutations (S13A and G10A) have an effect on substrate hydrolysis, and the influence is stronger on k_{cat} than on K_m. In particular in the AglA-S13A mutant K_m is slightly increased compared to the wild type enzyme whereas k_{cat} is reduced more than six-fold. This finding indicates that NAD^+ might be involved not only in substrate binding but also directly or indirectly in differential transition state stabilization.

In conclusion, the mutagenesis data reported here for the α-glucosidase AglA of *T. maritima* suggest that the highly conserved GXGS sequence motif of AglA and probably of all GHF4 enzymes is indeed involved in binding the cofactor NAD^+. The results of this work thus support the assumption that the N-terminal sequences of all GHF4 enzymes may adopt a Rossmann fold-like three-dimensional structure which could play an important role for the overall structure and/or catalytic mechanism of these unusual cofactor-dependent glycosidases.

Acknowledgements: The authors are grateful to Dr. R. Sterner (University of Cologne) for critical reading of the manuscript. The technical assistance of U. Ludwig is gratefully acknowledged. This work was supported by the Deutsche Forschungsgemeinschaft (Li398/6-3) and the Fonds der Chemischen Industrie.

References

[1] Henrissat, B. (1991) Biochem. J. 280, 309–316.
[2] see http://afmb.cnrs-mrs.fr/–cazy/CAZY/
[3] Burstein, C. and Kepes, A. (1971) Biochim. Biophys. Acta 230, 52–63.
[4] Raasch, C., Streit, W., Schanzer, J., Bibel, M., Gosslar, U. and Liebl, W. (2000) Extremophiles 4, 189–200.
[5] Zverlov, V., Velikodvorskaya, G. and Liebl, W., unpublished results.
[6] Thompson, J., Ruvinov, S.B., Freedberg, D.I. and Hall, B.G. (1999) J. Bacteriol. 181, 7339–7345.
[7] Bouma, C.L., Reizer, J., Reizer, A., Robrish, S.A. and Thompson, J. (1997) J. Bacteriol. 179, 4129–4137.
[8] Thompson, J., Pikis, A., Ruvinov, S.B., Henrissat, B., Yamamoto, H. and Sekiguchi, J. (1998) J. Biol. Chem. 273, 27347–27356.
[9] Thompson, J., Robrish, S.A., Immel, S., Lichtenthaler, F.W., Hall, B.G. and Pikis, A. (2001) J. Biol. Chem. 276, 37415–37425.
[10] Bibel, M., Brettl, C., Gosslar, U., Kriegshäuser, G. and Liebl, W. (1998) FEMS Microbiol. Lett. 158, 9–15.
[11] Rossmann, M.G., Liljas, A., Brändén, C.-I. and Banaszak, L.J. (1975) In: The Enzymes, Vol. 11, Part A (Boyer, P.D., Ed.), pp. 61–102, Academic Press, New York.
[12] Bellamacina, C.R. (1996) FASEB J. 10, 1257–1269.
[13] Sambrook, J., Fritsch, E.F. and Maniatis, T. (1989) Molecular Cloning: A Laboratory Manual, 2nd edn., Cold Spring Harbor Laboratory Press, Cold Spring Harbor NY.
[14] Pace, C.N., Vajdos, F., Fee, L., Grimsley, G. and Gray, T. (1995) Protein Sci. 4, 2411–2423.
[15] Wierenga, R.K., de Maeyer, M.C.H. and Hol, W.G.J. (1985) Biochemistry 24, 1346–1357.
[16] Scrutton, N.S., Berry, A. and Perham, R.N. (1990) Nature 343, 38–43.
[17] Schmid, F.X. (1997) In: Protein Structure: A Practical Approach (Creighton, T.E., Ed.), pp. 261–298, IRL Press, Oxford.